Electronic Supplementary Information

Energy Harvesting of Fully-Flexible Magnetoelectric Composites using a Piezoelectric P(VDF-TrFE) and Magnetostrictive $CoFe_2O_4$ Nanofiber

Chaeyoung Nam[a], Yujin Na[a], Sung Cheol Park[a], Hyunseung Kim[b], Chang Kyu Jeong[b], Geon-Tae Hwang[c,*], and Kwi-Il Park[a,*]

[a] *School of Materials Science and Engineering, Kyungpook National University, 80 Daehak-ro, Buk-gu, Daegu 41566, Republic of Korea*

[b] *Division of Advanced Materials Engineering, Jeonbuk National University, Jeonju, Jeonbuk 54896, Republic of Korea*

[c] *Department of Materials Science and Engineering, Pukyong National University, Busan 48513, Republic of Korea*

*CORRESPONDING AUTHORS

Geon-Tae Hwang

E-mail: gthwang@pknu.ac.kr, (Phone) +82-51-629-6362

Kwi-Il Park

E-mail: kipark@knu.ac.kr, (Phone) +82-53-950-5564

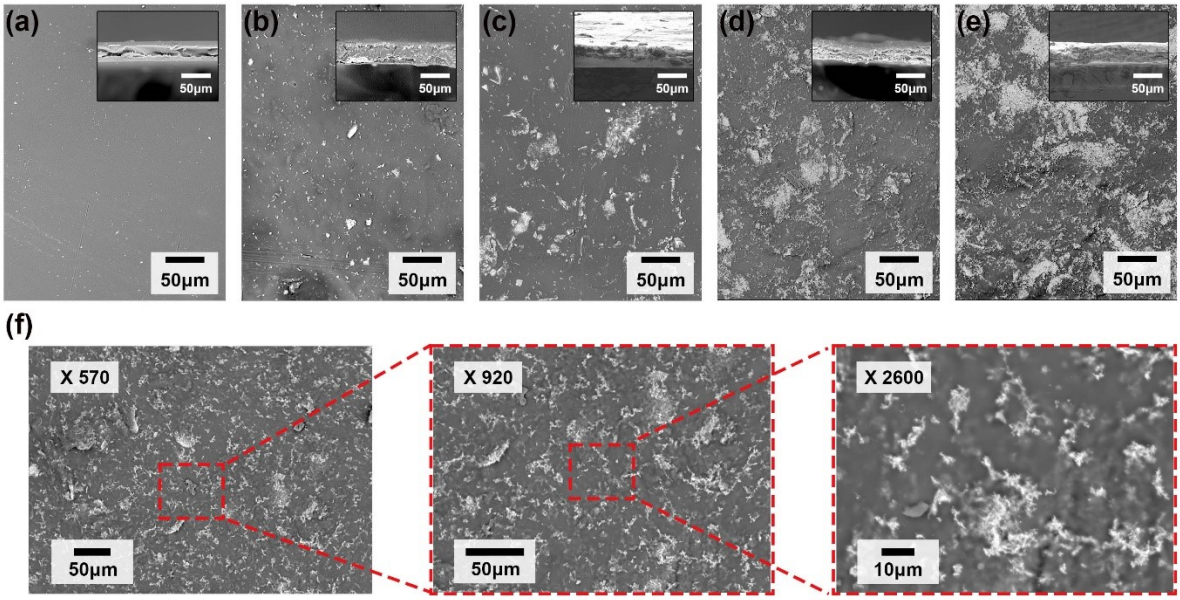

Fig. S1. (a-e) Top surface images of pure PI film and CFO/PI composite films with various CFO concentration. In the composite, dark part is PI polymer and bright part is distribution of CFO nanofibers. Each insets show that the fabricated films have a uniform thickness of 25 μm. (f) Top surface images of a CFO40/PI film obtained at various magnification (x570, x920, and x2600).

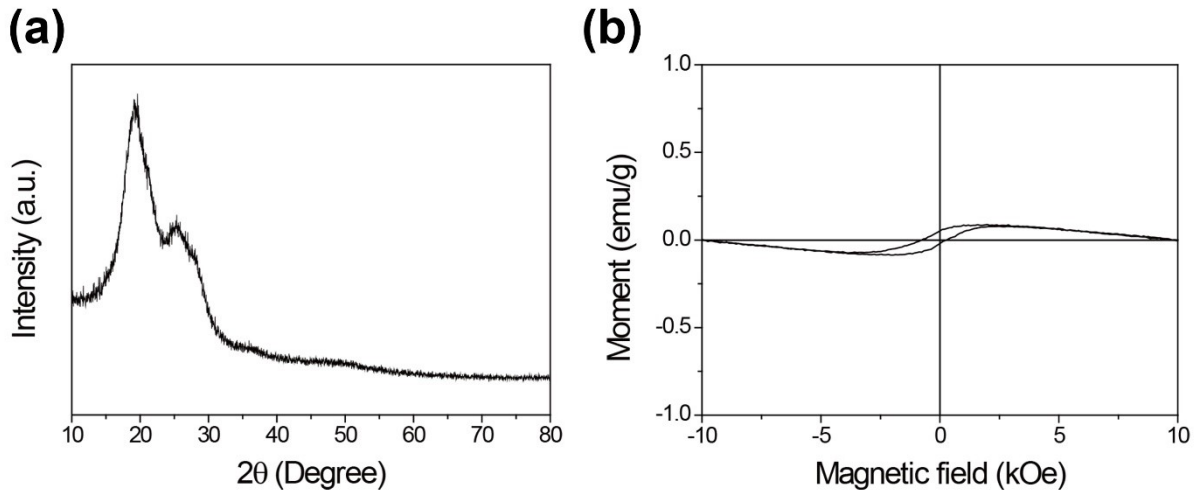

Fig. S2. (a) XRD diffraction pattern and (b) VSM analysis result of pure PI film after annealing process. Due to the non-magnetic nature of PI, the plot does not exhibit a hysteresis shape.

Determination of β phase content and piezoelectric charge coefficient of P(VDF-TrFE) film

The crystallized phase composition of P(VDF-TrFE) film was quantitatively identified by Fourier-transform infrared (FT-IR) analysis. As shown in Fig. S3a, the presence of three intensive absorption peaks at 844, 1286, and 1400 cm^{-1} are associated with the polar β phase of P(VDF-TrFE), while nonpolar α phase appears as negligible band at 766 cm^{-1}. Based on these results, the relative β phase fraction [F(β)] was obtained by the equation of Bear-Lambert law[S1, S2], as follows:

$$F(\beta) = \frac{A_\beta}{\left(\frac{K_\beta}{K_\alpha}\right)A_\alpha + A_\beta} \times 100\%$$

where A_α and A_β are the absorbances at 766 and 840 cm^{-1} and K_α and K_β are the absorption coefficients whose values are 6.1×10^4 and 7.7×10^4 $cm^2\ mol^{-1}$, respectively. The calculated electroactive β phase content was about 88.2 %, indicating well-crystallized properties of piezoelectric P(VDF-TrFE).

The piezoelectric charge coefficient (d_{33}) of the P(VDF-TrFE) was directly evaluated via piezoresponse force microscopy (PFM), as illustrated in Fig. S3b. After poling the sample under the electric field of 300 kV cm^{-1}, we performed the PFM analysis 10 times to ensure the reproducibility and derived piezoresponse displacement versus bias DC voltage plots.[S3, S4] By accurately calculating the slope of plots, d_{33} values for each plot were listed in Table S1. The average d_{33} of 55.44 pm V^{-1} confirms the high quality of fabricated P(VDF-TrFE) film.[S5]

References

[S1] J. Li, C. Zhao, K. Xia, X. Liu, D. Li and J. Han, *Appl. Surf. Sci.*, 2019, **463**, 626-634.

[S2] S.-R. Kim, J.-H. Yoo and J.-W. Park, *ACS Appl. Mater. Interfaces*, 2019, **11**, 15088-15096

[S3] S. S. Ham, G.-J. Lee, D. Y. Hyeon, Y.-g. Kim, Y.-w. Lim, M.-K. Lee, J.-J. Park, G.-T. Hwang, S. Yi, C. K. Jeong and K.-I. Park, *Compos. B. Eng.*, 2021, **212**, 108705.

[S4] C. Baek, J. H. Yun, J. E. Wang, C. K. Jeong, K. J. Lee, K.-I. Park and D. K. Kim, *Nanoscale*, 2016, **8**, 17632.

[S5] V. Bhavanasi, D. Y. Kusuma and P.S. Lee, *Adv. Energy Mater.*, 2014, **4**, 1400723.

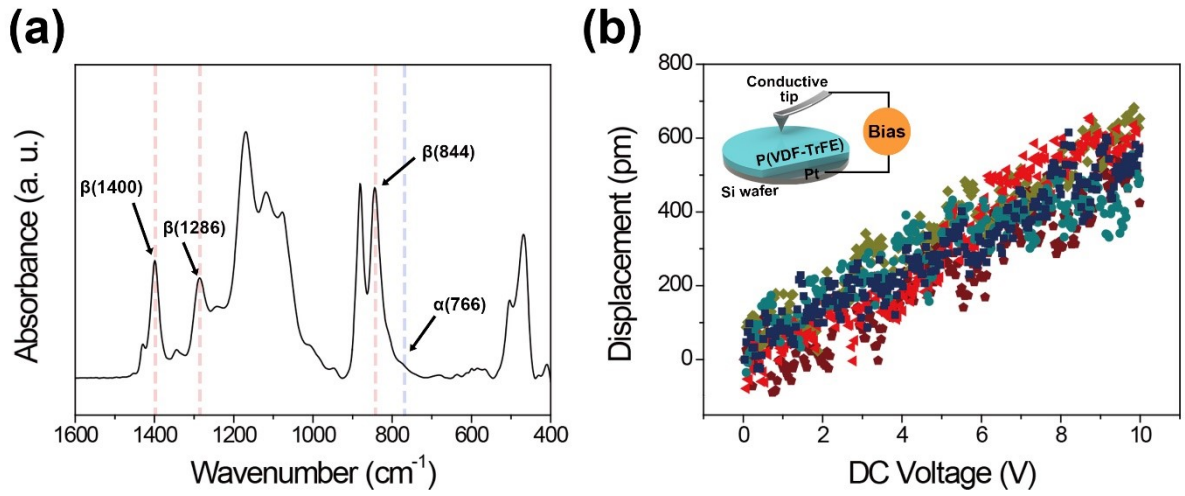

Fig. S3. (a) FT-IR spectra and (b) PFM analysis of piezoelectric P(VDF-TrFE) film.

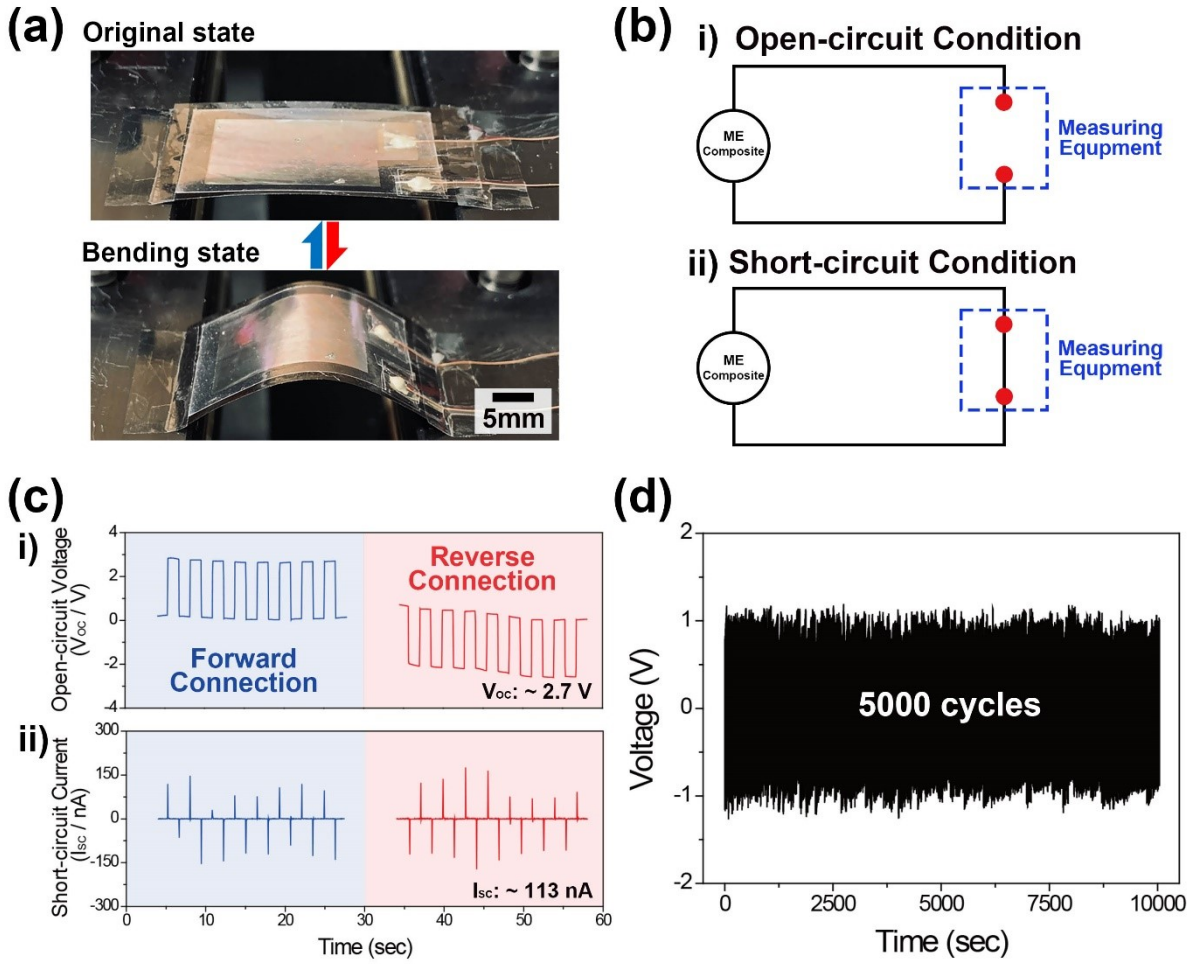

Fig. S4. (a) Photographs of the ME composite in original and bending states during piezoelectric energy conversion. (b) Circuit diagrams of open-circuit and short-circuit conditions to measure output voltage and current signals, respectively. (c-i) Open-circuit voltage and (c-ii) short-circuit current signals generated from ME composite in forward and reverse connections. (d) Mechanical stability test results under continuous bending of 5,000 cycles.

Explanation of measurement results of open-circuit voltage and short-circuit current generated from P(VDF-TrFE) film

The voltage signal generated from the flexible piezoelectric energy harvester was measured under an open-circuit condition (theoretically infinite-resistance state). After the bending motion of piezoelectric harvester, the generated electric charges from the harvesting device could be store in its top and bottom metal electrodes of MIM structure like a conventional capacitor, which could be presented as sudden rising and subsequent maintaining shape of voltage signal on the measuring electrometer. On the other hand, the current signal generated from the flexible harvester was measured under a short-circuit condition (theoretically zero-resistance state). After the bending motion of piezoelectric harvesting device, the generated whole electric charges could be instantaneously pass through the measuring electrometer, which could be presented as sudden rising and subsequent steep decaying of current signal like a peak shape during the measuring process of electrometer. As a result, the totally different resistance state between open-circuit and short-circuit conditions could make this greatly different waveform between voltage and current output signals.

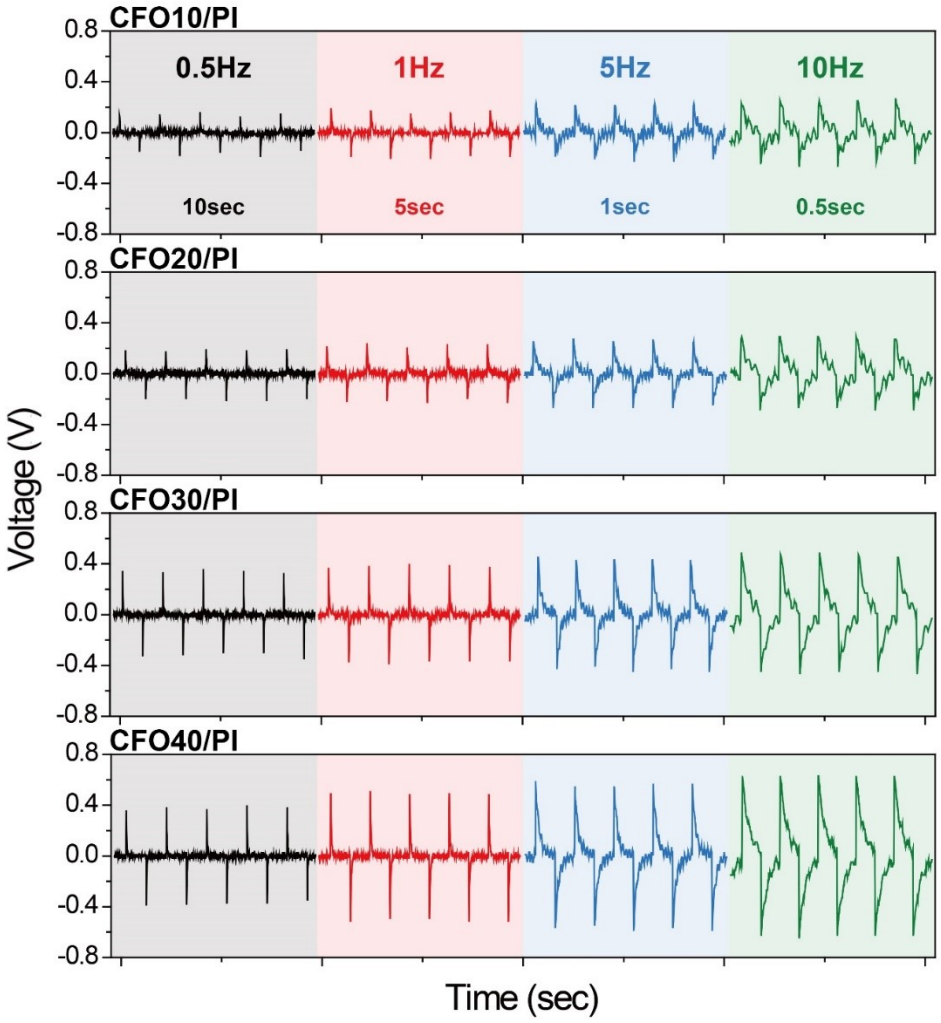

Fig. S5. The output voltage signals of flexible ME composites with various CFO concentration from 10 to 40 wt% at frequency ranging of 0.5 to 10 Hz. The highest voltage for all composites is achieved at 10 Hz.

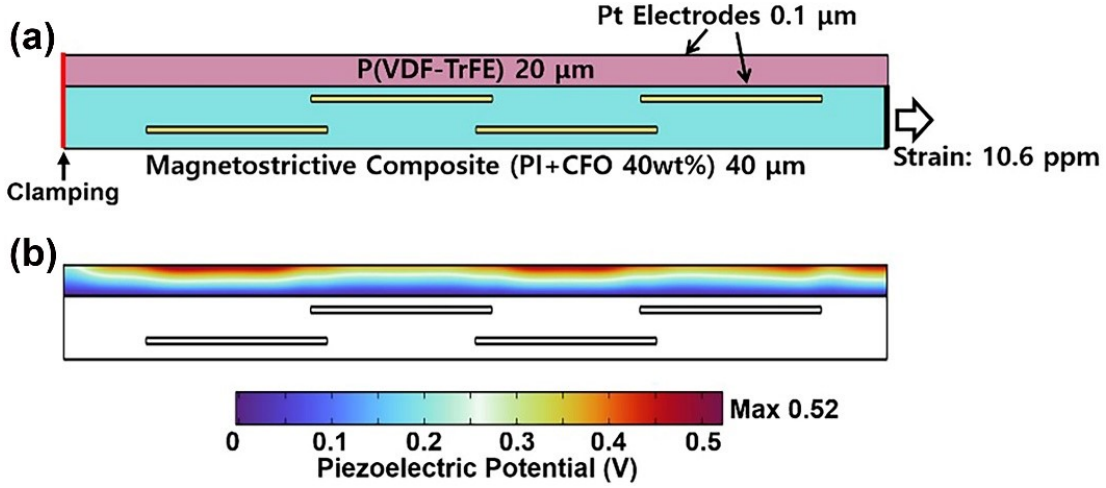

Fig. S6. A simulation model of ME composite harvester (a) and calculated piezopotential distribution inside the P(VDF-TrFE) (b) to estimate magnetostriction of magnetostrictive composite. The estimated tensile strain is 10.6 ppm on magnetostrictive composite to generate 0.52 V at P(VDF-TrFE) layer.

Table S1. PFM measurement results of piezoelectric P(VDF-TrFE) film after poling process.

Data point	d_{33} [pm V^{-1}]	Standard Error	R^2
Spot 1	53.65	1.40	0.90
Spot 2	60.46	1.27	0.91
Spot 3	57.25	1.25	0.89
Spot 4	57.96	0.99	0.93
Spot 5	54.60	1.24	0.88
Spot 6	52.36	1.15	0.94
Spot 7	54.53	1.09	0.94
Spot 8	55.31	1.15	0.92
Spot 9	51.82	1.19	0.82
Spot 10	56.42	1.01	0.91

Table S2. Comparison of the magnetoelectric voltage, power, and α_{ME} with recently reported ME composites

Material	Filler [wt%]	Voltage [mV]	Power [nW]	Year
P(VDF-TrFE)/ $NiFe_2O_4$ NPs	1	1400	-	2020[S6]
P(VDF-TrFE)/ $CoFe_2O_4$ NPs	20	1.1	-	2021[S7]
PVDF/$NiFe_2O_4$	7	17.45	400	2022[S8]
PVDF/$CoFe_2O_4$	10	18.87	930	2022[S9]
P(VDF-TrFE)/ $CoFe_2O_4$ NFs	40	520	6.61	**This work**

References

[S6] S. K. Ghosh, K. Roy, H. K. Mishra, M. R. Sahoo, B. Mahanty, P. N. Vishwakarma and D. Mandal, *ACS Sustain. Chem. Eng.*, 2019, **8**, 864-873.

[S7] X. Mu, H. Zhang, C. Zhang, S. Yang, J. Xu, Y. Huang, J. Xu, Y. Zhang, Q. Li, X. Wang, D. Cao and S. Li, *J. Mater. Sci.*, 2021, **56**, 9728-9740.

[S8] L. Paralı, Ç. E. D. Dönmez, M. Koç and S. Aktürk, *Curr. Appl. Phys.*, 2022, **36**, 143-159.

[S9] M. Koç, Ç. E. D. Dönmez, L. Paralı, A. Sarı and S. Aktürk, *J. Mater. Sci: Mater. Electron.*, 2022, **33**, 8048-8064.